Functional Significance of the Conformational Dynamics of the N-Terminal Segment of Secreted Phospholipase A2 at the Interface†

Badri P. Maliwal,*,‡,§ Bao-Zhu Yu,§ Henryk Szmacinski,‡ Thomas Squier,‡ Jan van Binsbergen,⊥ Arend J. Slotboom,⊥ and Mahendra K. Jain*,§

Center for Fluorescence Spectroscopy, Department of Biological Chemistry, University of Maryland Medical School, Baltimore, Maryland 21201, Department of Chemistry, University of Delaware, Newark, Delaware 19716, and Department of Biochemistry, Rijksuniversiteit, Padualaan 8, Utrecht, The Netherlands

Received August 17, 1993; Revised Manuscript Received December 10, 1993®

ABSTRACT: The kinetic and fluorescence properties of several pig pancreatic phospholipase A_2 (PLA2) with substitutions and deletions in the N-terminal region and of tyrosines 52 and 73 are characterized. The substitutions Ala-1-D-Ala or -Gly, Trp-3-Phe, Gln-4-Nle, Arg-6-Glu, Tyr-52-Phe, and Tyr-73-Phe had at the most only a modest effect on the interfacial catalytic activity on the anionic interface to which they bind with high affinity. The observed rate of hydrolysis in the scooting mode by deletion mutants lacking one or more successive residues from the N-terminal region was lower by 50–95%. Detailed kinetic analysis of the deletion mutant lacking Ala-1 (des-1-AMPA) showed that the 50% decrease in the rate is due to a 5-fold increase in the interfacial Michaelis–Menten parameter, K_M*, without a significant change in k_{cat}. These results and direct measurements show that the primary effect of Ala-1 deletion is to lower the affinity for the active site directed ligands. Although the affinity of these mutants for anionic interface remains the same as for the wild type, the affinity for zwitterionic neutral diluents is considerably lower. Significant differences in the fluorescence quantum yields and the heterogeneity in the frequency-domain fluorescence intensity decays of these enzymes suggest that both in solution and at the interface the N-terminal region is an ensemble of conformations rather than a discrete state. Additional results suggest that the interfacial microenvironment of Trp-3 in des-1-AMPA is more polar and Trp-3 is more accessible to quenching by acrylamide. This indicates incomplete desolvation of the microinterface in case of des-1-AMPA. The frequency-domain anisotropy decays of Trp-3 indicate that the N-terminal region of free PLA2 is somewhat rigid and becomes flexible as Ala-1 and Leu-2 are deleted. On the other hand, on DTPM vesicles, the N-terminal region is essentially rigid in PLA2 and des-1-AMPA, and it is only modestly flexible in bound des-1,2-AMPA. These observations demonstrate a ligand-induced rigidification of the N-terminal region of the E*I form of PLA2, and it is surprising that such a rigidification is observed in the absence of Ala-1. Taken together these results show that Ala-1 and the associated hydrogen-bond network affect the binding of an active site directed ligand via its role in desolvation of the interface but without a significant effect on the chemical step of the catalytic turnover cycle.

Interfacial catalytic behavior of phospholipase A_2 (PLA2)[1] is adequately described by the reaction sequence:

$$E \overset{K_d}{\rightleftarrows} E^* + S \underset{k_{-1}}{\overset{k_1}{\rightleftharpoons}} E^*S \overset{k_{cat}}{\rightarrow} E^* + P$$

where the binding of the enzyme from the aqueous (E) to the interface (E*) precedes the catalytic turnover, suggesting a separation of the steps of catalytic turnover cycle (Verheij et al., 1981; Volwerk & de Haas, 1982). A support for this dissection is provided by the fact that the E, E*, and E*L forms of the enzyme have distinct spectroscopic signatures (Jain & Maliwal, 1993). A functional separation of these two events implies not only an increased residence time and enhanced catalytic processivity of the enzyme at the interface (Jain et al., 1986a) but it also provides a functional basis for understanding interfacial activation (Jain et al., 1993). Such analysis has provided a basis for deconvolution of the interfacial rate and equilibrium parameters (Berg et al., 1991). The importance of obtaining insights into the structural basis for the intrinsic functional differences between the E and E* forms

† This work was supported by Grant GM29703 (M.K.J.) from the National Institutes of Health. We thank Professor Joseph Lakowicz for use of the facilities of the Center for Fluorescence Spectroscopy at the University of Maryland supported by Grants RR08119 from the National Institutes of Health and Dir-8710401 from the National Science Foundation.

‡ University of Maryland Medical School.

§ University of Delaware.

⊥ Rijksuniversiteit.

® Abstract published in *Advance ACS Abstracts,* March 15, 1994.

[1] Abbreviations: The kinetic and equilibrium constants are defined conventionally except for the fact that the parameters marked with an asterisk relate to the equilibria at the interface. For example, K_L and K_L* values are the equilibrium dissociation constants for the EL and E*L complexes, where L is a substrate, product or inhibitor; $X_I(50)$ is the mole fraction required for 50% inhibition; v_o, is the measured initial rate at mole fraction = 1 of the substrate at the interface; k_{cat} is the calculated rate at the saturating substrate mole fraction based on the value of the interfacial Michaelis–Menten constant, K_M*. K_d, dissociation constant for E* to E; K_d^I, dissociation constant for E*I to EI; AMPA, ϵ-amidinated PLA2 from pig pancreas; deoxy-LPC, 1-hexadecylpropanediol-3-phosphocholine; des-1-AMPA, AMPA without the alanine at the N-terminus; des-1,2-AMPA, AMPA without Ala-1 and Leu-2 at the N-terminus; des-1,6-AMPA, AMPA without residues 1–6 at the N-terminus; des-1,8-AMPA, AMPA without residues 1–8 at the N-terminus; DMPM, dimyristoylglycero-*sn*-3-phosphomethanol; DTPM, ditetradecylglycero-*sn*-3-phosphomethanol; E, E*, and E*L, the enzyme in the aqueous phase, the enzyme at the interface, and the enzyme–ligand complex at the interface; MJ33, 1-hexadecyl-3-(trifluoroethyl)-*rac*-glycero-2-phosphomethanol; MJ72, 1-octyl-3-(trifluoroethyl)-*rac*-glycero-2-phosphomethanol; PLA2, native phospholipase A2 from pig pancreas unless stated otherwise.

0006-2960/94/0433-4509$04.50/0

is obvious, and such attempts may be viewed in terms of two different hypotheses elaborated below.

According to the "enzyme conformation" theory apparently higher catalytic turnover by E* is the result of a discrete conformational transition that occurs on the binding of the enzyme to the interface (Volwerk & de Haas, 1982). Putatively, the H-bond network involving Ala-1 along with the N-terminal helix stabilizes the E* form (Dijkstra et al., 1981, 1983). In the X-ray crystal structures of bovine and porcine PLA2 and their complexes with inhibitors, the α-NH_3^+ group of Ala-1 is hydrogen bonded to nearly invariant Gln-4 and Glu(Asn)-71 and is linked by a structural water molecule to invariant residues Tyr-52, Tyr-73, and Asp-99, the last residue being part of the "catalytic triad". Hydrogen bonds with the carbonyl from the backbone of residues Pro-68 and Glu-71 are also implicated in this network. In addition, residues Leu-2, Phe-5, and Ile-9 form a part of the wall of the active-site cavity (Scott et al., 1990; Thunnissen et al., 1990). Multidimensional NMR studies of E and E*I complex indicate that the hydrogen-bond network is fully formed only when an active site directed ligand binds to the enzyme at the interface (Dekker et al., 1991a,b; Peters et al., 1992). Thus, according to this hypothesis, the interfacial activation of the enzyme is brought about by the formation of this hydrogen-bond network (Volwerk & de Haas, 1982).

Several observations raise doubt about a crucial role for such a discrete two-state conformational transition and the H-bond network: (a) The remarkable similarity in the catalytic surfaces among evolutionarily divergent PLA2 and between E and EI complexes in the crystal structures suggests that the optimal active-site architecture is already present in the free enzyme (Scott et al., 1990; Thunnissen et al., 1990). (b) The affinity of PLA2 for the cofactor calcium is essentially the same for the E and E* forms (Jain et al., 1991a). (c) The role of hydrogen bonds involving tyrosines at 52 and 73 in the interfacial catalysis is virtually ruled out by normal enzyme activity observed with corresponding phenylalanine mutants of bovine (Dupureur et al., 1992a) and porcine (Kuipers et al., 1990) PLA2. On the basis of such considerations and dynamic fluorescence results, it has been suggested that the N-terminal segment of the E form of PLA2 exists as an ensemble of conformations (Jain & Maliwal, 1993). Upon binding to an interface (E to E*), the N-terminal segment of PLA2 becomes more rigid, representing a narrower ensemble of perhaps the optimally active conformation. Moreover, desolvation of the interface associated with the formation of E*L also plays a significant role in the enhanced interfacial activity (Jain & Vaz, 1987; Ramirez & Jain, 1991) due to an increased affinity of the bound enzyme for the substrate (Jain et al., 1993).

In this paper we report studies designed to evaluate the role of the N-terminal region. The kinetic and equilibrium binding properties of several mutants of pig pancreatic PLA2 with substitution and deletion in the N-terminal region were determined. Parallel fluorescence studies were also carried out to characterize the conformational dynamics of the N-terminal region and thus provide a structural basis for the observed functional changes. These results show that the H-bonded network associated with Ala-1 is not necessary for the chemical step of the catalytic cycle, but it plays an important role in the binding of active site directed ligands to the enzyme at the interface. Although the affinity of the enzyme for the anionic interface is not noticeably altered by these mutations, the affinity for binding to zwitterionic interfaces does decrease significantly. In fact, this dissection of the three steps provides a rationale for the loss of catalytic activity of these mutants on zwitterionic interfaces (Slotboom & de Haas, 1975; Van Scharrenburg et al., 1984a,b).

MATERIALS AND METHODS

All reagents, proteins, and phospholipids used here were of better than 99% purity as checked by thin-layer chromatography or HPLC in appropriate solvent systems. Methods for the preparation of lipids (Jain et al., 1986a), neutral diluents (Jain et al., 1991a,b), competitive inhibitors (Jain et al., 1991c), native, alkylated, amidinated, and semisynthetic PLA2 (Van Scharrenburg et al., 1984a,b) have been described. Tyr-52-Phe, and Tyr-73-Phe mutants of the porcine PLA2 were kindly provided by Professor Verheij. The general protocols for monitoring the steady-state fluorescence and acrylamide quenching (Jain et al., 1986b; Jain & Maliwal, 1985, 1993), for obtaining the steady-state rate of hydrolysis, v_o, expressed as turnover number, for interfacial catalysis in the scooting mode (Jain et al., 1991a,b), and for determining the rate and equilibrium parameters and the underlying analytical relations (Berg et al., 1991, Jain et al., 1991a, 1993; Yu et al., 1993) have been established. Uncertainties in the experimental values are less than 10%, and the standard deviations for the derived parameters were less than 30%.

All spectroscopic measurements were made in 10 mM Tris, 0.5 mM $CaCl_2$ at pH 8.0 and 24 °C. Unless stated otherwise, for the steady-state fluorescence measurements the excitation wavelength was 292 nm and the protein concentration was between 3 and 10 μM with no noticeable inner filter effects. Steady-state fluorescence spectra were obtained on an SLM 4000 or 4800S spectrophotometer. The ultraviolet absorption spectra were measured on a HP8452 spectrophotometer equipped with a diode array detector, and the protein concentration was between 20 and 35 μM.

The dynamic fluorescence measurements were performed on a 10-GHz frequency-domain harmonic content fluorometer as described (Laczko et al., 1990). The harmonic content of a rhodamine 6G dye laser, synchronously pumped with a mode-locked argon ion laser, cavity dumped at 3.75 MHz, and frequency-doubled to 295 nm was used as an excitation source. The emission was observed through Corning 0–54 and 7–54 filters which provided a broad emission window. The protein concentration was between 20 and 50 μM, and a 4-mm pathlength cuvette was used. The frequency responses of the emission intensity decays were analyzed by nonlinear least-squares fitting routines as a sum of exponentials (Lakowicz et al., 1984):

$$I(t) = \sum \alpha_i \exp(-t/\tau_i) \quad (1)$$

where α and τ are amplitudes and the associated lifetime components. The average life time $\langle\tau\rangle$ was computed as

$$\langle\tau\rangle = \sum \alpha_i \tau_i \quad (2)$$

All related intensity decays were globally analyzed for three common and one variable exponential decay components. Such analysis gave same χ_R^2 values as separate, unrestrained analysis of each file but significantly reduced the uncertainty in the resolved parameters.

The anisotropy decays $[r(t)]$ were analyzed as a sum of exponentials as follows (Weber, 1977; Maliwal & Lakowicz, 1986):

$$r(t) = \sum_i r_i \exp(-t/\theta_i) \quad (3)$$

Table 1: Catalytic Turnover Numbers (v_o) and Relative Quantum Yields (RQY) of PLA2, Semisynthetic AMPA, and the Tyr Mutants in the Scooting Mode Assay with DMPM

mutant	v_o (s^{-1})	RQY PLA2	RQY PLA2-DTPM
PLA2	270	1	1.76
pro-PLA2	0.8	2.13	1.95
AMPA	270	1.04	1.78
Ala-1-Gly-AMPA	230	1.86	0.9
Ala-1-D-Ala-AMPA	270	1.88	0.82
des-1-AMPA	120	1.84	1.02
des-1,2-AMPA	9	2.64	0.87
des-1,6-AMPA	25	<0.03	<0.03
des-1,8-AMPA	17	<0.03	<0.03
Trp-3-Phe-AMPA	200	<0.05	<0.05
Gln-4-Nle-AMPA	180	0.90	0.61
Arg-6-Glu,Gly-7-Ala-AMPA	230	1.65	1.85
Gly-7-Ala-AMPA	250	1.09	1.90
Tyr-52-Phe-PLA2	290	1.14	1.69
Tyr-73-Phe-PLA2	290	1.41	1.91

Table 2: Equilibrium Dissociation Constants[a] for PLA2 and Des-1-AMPA

	PLA2	des-1-AMPA
K_{Ca}	0.32 mM	0.25 mM
K_{Ca}*	0.26 mM	0.13 mM
K_S* (DTPM)	0.030	>0.1
K_P* (DMPM)	0.026	>0.1
K_M* (DMPM)	0.35	2.0
X_I(50) MJ33-rac	0.006	0.04
K_I* MJ33-rac	0.0016	0.028
v_o (s^{-1})	270	120
k_{cat} (s^{-1})	370	360

[a] Values are given in mole fraction unless shown otherwise. The uncertainty in these values is 30%.

where θ_i are the rotational correlation times, r_i are associated amplitudes, and $\sum r_i$ give the zero-time or the limiting anisotropy, r_o. The uncertainties in the recovered intensity and anisotropy decay parameters are at a 67% confidence limit level and take into account correlations among the parameters (Johnson, 1983).

RESULTS

Catalytic Activity of the Mutants. The steady-state catalytic turnover numbers for the hydrolysis of anionic DMPM vesicles in the highly processive scooting mode (Berg et al., 1991; Jain et al., 1991a) by several mutants of PLA2 are summarized in Table 1. In this assay system v_o values for PLA2 and its ε-amidinated derivative (AMPA) are 270 s^{-1}, and comparable values were obtained for virtually all substitution mutants (Ala-1-D-Ala or Gly, Trp-3-Phe, Gln-4-Nle, Arg-6-Glu, Gly-7-Ala, Tyr-52-Phe, and Tyr-73-Phe). On the other hand, deletion of Ala-1 (des-1-AMPA) reduced the rate to 120 s^{-1}. Further deletion of Leu-2 lowered the rate to 9 s^{-1}. It is remarkable that the turnover numbers for des-1,6-AMPA and des-1,8-AMPA are still about 15 s^{-1}, that is about 20 times higher than those observed for the pro-enzyme (less than 1 s^{-1}). The kinetic and structural basis for a lower catalytic turnover rate by des-1-AMPA was developed on the basis of the studies described below.

Kinetic Characterization of Des-1-AMPA. The interfacial rate and equilibrium parameters for des-1-AMPA are compared with those for the WT PLA2 in Table 2. The dissociation constant for calcium in the aqueous phase or the interface were comparable for the two enzymes. However, the affinities for several active site directed anionic ligands (products, competitive inhibitor, substrate analog) were lower by a factor

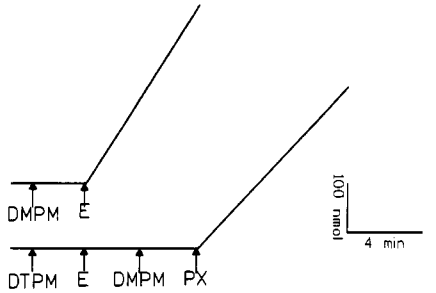

FIGURE 1: Reaction progress curves for the hydrolysis of (top) DMPM (0.3 mM) vesicles by des-1-AMPA in the presence of polymyxin B (20 μg); (bottom) the enzyme was added to DTPM (0.08 mM) vesicles followed by DMPM (0.3 mM) vesicles and then polymyxin B.

of 10 for the deletion mutant. The apparently lower affinity for the binding of the substrate is also reflected in the value for K_M* for DMPM, which increases from 0.35 mole fraction for PLA2 to 2.0 mole fraction for des-1-AMPA. Thus the calculated value of $k_{cat} = k_2$ is about 360 s^{-1} for the deletion mutant compared to the value of 370 s^{-1} for PLA2. The basis for a lower affinity for the substrate may also be dissected because the effect of the 5-fold change in the value of K_M* corresponds to the change in the value of K_S*. By definition $K_M^* = (k_2 + k_{-1})/k_1$. For PLA2 the value of k_{-1} (=35 s^{-1}) is considerably smaller than the value of k_2 = 370 s^{-1} (Berg et al., 1991). Therefore, it may be argued that the main effect of the deletion of Ala-1 is on k_1, which would be lowered from 1300 s^{-1} in the wild type PLA2 to about 200 s^{-1} for des-1-AMPA.

Although we have not investigated in detail, lower v_o values for deletion mutants involving Leu-2 and up to Met-8 can also be rationalized on the basis of higher K_M* of 5–10 mol fraction. This is expected because Leu-2 and Phe-5 are part of the active-site cavity, and any disruption of the active site architecture would adversely affect both the binding to the active site and the chemical step.

Binding to the Anionic Interface. During catalytic turnover in the scooting mode, PLA2 does not dissociate from the interface (Jain et al., 1986a; Berg et al., 1991). Therefore the low turnover number for des-1-AMPA can also result if its residence time at the vesicle interface is lower. This is so because on the time-average basis the steps for the binding and dissociation of the enzyme from the interface also become a part of the catalytic cycle (Jain et al., 1986a,b; 1991b). To assess this possibility, des-1-AMPA bound to vesicles of the nonhydrolyzable ether analogue DTPM was exposed to the substrate (DMPM) vesicles. If there was any exchange of the bound enzyme with the excess vesicles, the DMPM vesicles would have been hydrolyzed. As shown in Figure 1 this is not the case. In fact, none of the deletion mutants showed any intervesicle hopping (results not shown). As also shown in Figure 1, des-1-AMPA bound to DTPM was readily transferred to DMPM vesicles in the presence of polymyxin B which promotes intervesicle transfer of phospholipids between these vesicles (Jain et al., 1991b). These results show that the deletion mutants as well as PLA2 bind to DMPM vesicles essentially irreversibly.

Binding to the Zwitterionic Interface. The dissociation constants for PLA2 and the two deletion mutants bound to micelles of deoxy-LPC are summarized in Table 3. It may be recalled that deoxy-LPC is a neutral diluent, i.e., although PLA2 binds to the interface of the aqueous dispersions of deoxy-LPC, this amphiphile has little affinity for the catalytic active site of the enzyme (Jain et al., 1991a,c; Dupureur et al., 1992a,b). The dissociation constant (K_d) for PLA2 bound

Table 3: Dissociation Constants (mM)[a] for the E (K_d) and E-MJ72 (K_d^I) Forms of PLA2, Des-1-AMPA, and Des-1,2-AMPA for Deoxy-LPC Micelles at 10 mM $CaCl_2$

parameter	PLA2	des-1-AMPA	des-1,2-AMPA
K_d (E* to E)	0.8	≫6	≫6
K_d^I (E*L to EL)	0.025	0.06	0.12

[a] Uncertainty in these values is less than 20%.

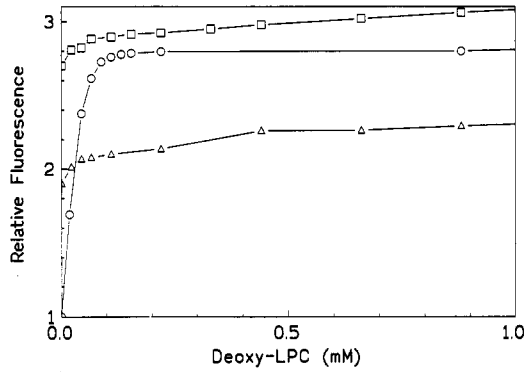

FIGURE 2: The fluorescence intensity of (circles) PLA2, (triangles) des-1-AMPA, and (squares) des-1,2-AMPA at 333 nm (ex. 292 nm) as a function of deoxy-LPC added in the presence of 0.2 mM MJ72.

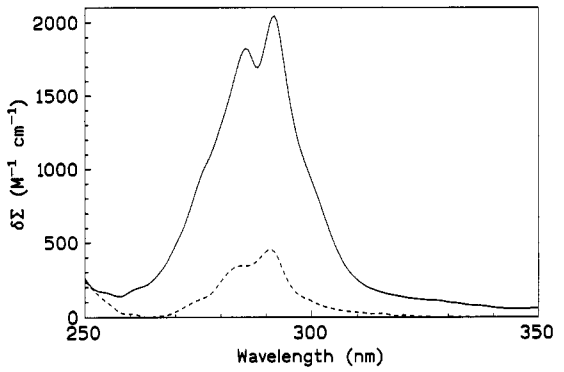

FIGURE 3: UV difference spectrum of (continuous line) PLA2 and (dashed line) des-1-AMPA obtained upon binding to 2 mM deoxy-LPC in the presence of 0.1 mM MJ33.

to deoxy-LPC micelle (E* to E) is about 0.8 mM. On the other hand, even up to 6 mM deoxy-LPC little or no change in the fluorescence intensity or anisotropy could be detected with des-1-AMPA or des-1,2-AMPA. This indicates that des-1-AMPA and des-1,2-AMPA have lost their affinity for the interface of the neutral diluent.

Also included in Table 3 are the K_d^I values (with MJ72) for the dissociation of the E*I from deoxy-LPC micelles to EI in the aqueous phase obtained from the titration curves of the type shown in Figure 2. The K_d^I values were 25, 60, and 125 μM for PLA2, des-1-AMPA, and des-1,2-AMPA, respectively. In the case of PLA2, essentially identical values were obtained in the presence of several other active site directed anionic and zwitterionic inhibitors (results not shown; however, see Jain et al., 1993). These results show that the differences among the K_d^I values are considerably smaller (5-fold) than the K_d values which are at least 100-fold higher for the deletion mutants.

UV Difference Spectra. The UV difference spectra obtained upon binding of MJ33 to PLA2 and des-1-AMPA in the presence of deoxy-LPC micelles are shown in Figure 3. These difference spectra are characterized by peaks at 292 and 284 nm, a shoulder around 300 nm, and a minor negative trough around the 260-nm region. The shape and the large amplitude of difference spectra indicate that Trp-3 has moved to an environment of lower polarity (Donovan, 1969; Jain & Maliwal, 1993). The difference spectrum for des-1-AMPA though similar in shape to that of WT is of substantially lower amplitude (2300 versus 450 M^{-1} cm^{-1}). On the basis of the K_d^I values, it can be shown that all of the enzyme is in the interface under these conditions. Also from the values of K_I^* for the dissociation of E*I to E* + I (Table 2), it can be calculated that more than 90% of PLA2 and little more than half of des-1-AMPA is in the E*I form. This suggests that the amplitude of the difference spectrum for des-1-AMPA is intrinsically smaller than that for PLA2. This indicates that the tryptophan is in a relatively more polar interface for the E*I form of des-1-AMPA compared to for PLA2. As elaborated elsewhere (Jain & Maliwal, 1993), the origin of this large amplitude difference spectrum lies in the desolvation of the microinterface of the E*L form driven by the binding of the ligand to the active site, which would suggest that deletion of Ala-1 affects the desolvation step associated with these interactions.

Steady-State Fluorescence Properties. The fluorescence quantum yields of PLA2 and the mutants are summarized in Table 1. The quantum yield of 0.039 for PLA2 in the aqueous phase is significantly lower than that of *N*-acetyltryptophanamide (=0.12). We also observed large variations in the quantum yields for the mutants. Deletion of Ala-1 or disruption of its α-NH_3^+ function as in the D-Ala-containing mutant resulted in significantly increased quantum yields. A further increase was observed on the deletion of Leu-2. These results are consistent with earlier studies (Van Scharrenburg et al., 1984a,b; Jain et al., 1986b), which suggested that protonated Ala-1 and Arg-6 are among the quenchers of Trp-3 fluorescence.

Quantum yields of PLA2 and mutants bound to DTPM vesicles are also summarized in the last column of Table 1. Upon binding to the anionic interface, there was a large increase in the quantum yield of PLA2 and its ϵ-amidinated derivative (Jain et al., 1986b). There was also an increase in the quantum yields of the Arg-6-Glu, Gly-7-Ala, Tyr-52-Phe, and Tyr-73-Phe mutants. The quantum yields were essentially similar for the E*I forms of all these mutants and PLA2. On the other hand, perturbation of the α-NH_3^+ function by substitution or deletion of Ala-1 or Gln-4 lowers the quantum yield of the E*I form. Collectively these results suggest that the fluorescence intensity of Trp-3 is significantly affected by the neighboring amino acids and that some of the quenching mechanisms present in PLA2 are eliminated upon the deletion of Ala–1 and Leu-2 in the solution (E form) as well as on the binding to the interface (E*I form). In conjunction with the intensity decay measurements described later in this paper, these results also suggest that the N-terminal segment exists as an ensemble of conformations.

Results of a detailed investigation of the fluorescence emission properties of PLA2 and the two deletion mutants are summarized in Table 4. Successive deletions of Ala-1 and Leu-2 shift the emission maxima to higher wavelengths for the enzyme in the E form (345, 348, and 352 nm) as well as the E*L form (333, 342, and 347 nm). The higher values of emission maxima suggest a more polar microenvironment for Trp-3 in the deletion mutants in E and E*I forms. The acrylamide quenching constants are also summarized in this table. Trp-3 is on the surface of the E form, and it is freely accessible to acrylamide. Upon binding to codispersions of deoxy-LPC and MJ72 (E*I form), a significant shielding, though to varying degrees, was observed by a factor of 10 and

Table 4: Fluorescence Emission Maxima and Acrylamide Bimolecular Quenching Constants of E and E*L Forms of PLA2s

	PLA2	des-1-AMPA	des-1,2-AMPA
E, λ_{max} (nm)	345	348	352
E*L, λ_{max} (nm) (deoxy-LPC.MJ33)	333	342	347
E*L, λ_{max} (nm) (DTPM)	333	343	347
k_q (M^{-1} s^{-1}) (DTPM)	≤0.4	1.9	3.6
k_q (M^{-1} s^{-1}) (deoxy-LPC.MJ72)	0.7	4.0	ND[a]

[a] ND, not determined. The bimolecular quenching constant for acrylamide quenching is 6.5 M^{-1} s^{-1} in the case of PLA2 and is comparable to that expected for an accessible surface-exposed residue (Jain & Maliwal, 1993).

3 for PLA2 and des-1-AMPA, respectively. Similarly, for these three enzymes on DTPM vesicles the relative decrease in acrylamide accessibility was approximately 20-, 4-, and 2-fold compared to that for the E forms. Overall, these results indicate decreased shielding to acrylamide and a more polar environment for Trp-3 in the deletion mutants at the interface.

Fluorescence Intensity Decays. The results from the multiexponential fits to frequencys-domain intensity decays of PLA2 and some of the AMPA are summarized in Table 5. Four decay components were needed to satisfactorily describe the frequency responses; the χ_R^2 values for the 3-component fit were 3-fold larger. Since the uncertainties are between 10 and 20%, it is the trend rather than the absolute values which are of importance here. The values of the four decay components from the global analysis were about 0.2, 0.7–1.1, 2.7, and 6.2 ns. For PLA2 the first two decay components comprise about 77% of the fluorescent population, while the longest lived component is about 4%. Deletion of Ala-1 (des-1-AMPA) resulted in a significant shift from the two shortest lived components to the longest lived one which increased from about 4% to almost 13%. Further removal of Leu-2 (des-1,2-AMPA) amplified these changes. The two shortest lifetimes now make up only 42% of the population, while the remaining two populations increase by almost 2-fold. These changes in the population are reflected in the average lifetime values of 1.12, 1.77, and 2.7 ns, respectively, for PLA2, des-1-AMPA, and des-1,2-AMPA. The trends in the average lifetime and the quantum yields are reasonably similar, suggesting that some of the quenching processes operative in PLA2 are diminished in these two semisynthetic derivatives. As suggested by anisotropy measurements described below, the Trp-3 in the two deletion mutants, being considerably more mobile, is able to minimize some of these quenching contacts.

The fluorescence lifetimes and amplitudes of the fluorescence decay from PLA2, des-1-AMPA, and des-1,2-AMPA at the DTPM interface are summarized in Table 6. Again four decay components of about 0.1, 0.7–1.0, 2.6, and 6.4 ns were required to obtain satisfactory fits, and the improvement in χ_R^2 value was less than 2-fold compared to that for three components. For PLA2 on DTPM vesicles the two shortest lifetime components make up about 58% of the population and the longest lived is about 4%. In the case of both des-1- and des-1,2-AMPA, a significant shift toward two shortest lifetimes occurs in DTPM complexes as they make up between 75 and 80% of the population, as is the case for the E form of PLA2. The values of the average lifetime of DTPM complexes are 1.6 ns in case of PLA2 and about 1.1 ns in the case of des-1- and des-1,2-AMPA.

There are several observations that can be made from these results. An increase in the steady-state intensity is reflected as a shift from two shortest lived components to longer lived ones in the intensity decays. The increase in the fluorescence intensity in the E forms is accompanied by an increase in the population of the 6.2-ns species, while in the E*DTPM the population of the 2.7-ns species increase. On the other hand, in the deletion mutants where the quantum yields decrease upon binding to DTPM, the shifts are toward the two short-lived components. It should also be noted that the intensity decays of Trp-3 at the ionic interface are significantly more heterogeneous than those reported for the enzyme bound to micelles of zwitterionic hexadecylphosphocholine (Ludescher et al., 1985; Kuipers et al., 1991), as well as the E*, E*I and E*P forms on deoxy-LPC (Jain & Maliwal, 1993). Such remarkable heterogeneity in the intensity decays of the E and E*L forms further suggests that the N-terminal region of PLA2 is an ensemble of conformations rather than a discrete state.

Anisotropy Decays of PLA2. The frequency-domain anisotropy decays of PLA2, des-1-AMPA, and des-1,2-AMPA and their DTPM complexes are summarized in Table 7. The anisotropy decays for the E forms could be satisfactorily described by two correlation times. The larger correlation time of about 6.0–6.5 ns reflects the overall motions of the protein, while the 0.15–0.25-ns component represents the local segmental motions of the region where the indole ring is located. The local motions in PLA2 make up less than 20% of the limiting anisotropy, suggesting a somewhat rigid N-terminal segment. Removal of Ala-1 (des-1-AMPA) resulted in an increase in the motional freedom of Trp-3 as the local motions

Table 5: Frequency-Domain Fluorescence Intensity Decays of PLA2 and Some of the Semisynthetic Derivatives

	α_i				τ_i (ns)					
	α_1	α_2	α_3	α_4	τ_1	τ_2	τ_3	τ_4	$\langle\tau\rangle$	χ_R^2
PLA2	0.391 ± 0.043	0.378 ± 0.038	0.191 ± 0.018	0.040 ± 0.010	0.16 ± 0.05	0.76 ± 0.12	2.73 ± 0.28	6.17 ± 0.35	1.12	0.54
des-1-AMPA	0.360 ± 0.050	0.336 ± 0.028	0.170 ± 0.040	0.138 ± 0.020		1.13 ± 0.16			1.77	
des-1,2-AMPA	0.258 ± 0.041	0.157 ± 0.031	0.307 ± 0.041	0.278 ± 0.041		0.75 ± 0.20			2.74	

Table 6: Frequency-Domain Trp-3 Intensity Decays of Anionic Lipid Complexes of PLA2 and Some Semisynthetic Derivatives

	α_i				τ_i (ns)					
	α_1	α_2	α_3	α_4	τ_1	τ_2	τ_3	τ_4	$\langle\tau\rangle$	χ_R^2
PLA2-DTPM	0.321 ± 0.036	0.264 ± 0.031	0.375 ± 0.032	0.040 ± 0.012	0.13 ± 0.05	0.80 ± 0.12	2.57 ± 0.18	6.37 ± 0.38	1.59	1.13
des-1-AMPA-DTPM	0.635 ± 0.046	0.158 ± 0.028	0.155 ± 0.032	0.052 ± 0.010		0.96 ± 0.18			0.98	
des-1,2-AMPA-DTPM	0.421 ± 0.064	0.341 ± 0.041	0.199 ± 0.028	0.039 ± 0.010		0.70 ± 0.08			1.06	

Table 7: Frequency-Domain Anisotropy Decay Parameters of WT and Semisynthetic PLA2 and Their Anionic Lipid Complexes at 25 °C[a]

sample	r_i			θ_i (ns)			r_0 (295 nm)	χ_R^2
	r_1	r_2	r_3	θ_1	θ_2	θ_3		
				Free Enzyme				
PLA2	0.028 ± 0.004		0.195 ± 0.003	0.24 ± 0.08		6.3 ± 0.26	0.223 ± 0.004	1.02
des-1-AMPA	0.070 ± 0.018		0.155 ± 0.003	0.15 ± 0.07		6.2 ± 0.16	0.225 ● 0.012	0.38
des-1,2-AMPA	0.067*	0.028 ± 0.012	0.130 ± 0.010	<0.15*	1.2 ± 0.48	6.2 ± 0.8	0.225*	0.70
				Enzyme–DTPM Complex				
PLA2	0.011 ± 0.004		0.198 ± 0.003	0.40 ± 0.19		30.6 ± 2.7	0.209 ± 0.004	0.24
des-1-AMPA	0.028**		0.182 ± 0.005	<0.4**		18.3 ± 5.0	0.210**	1.06
des-1,2-AMPA	0.048**		0.162 ± 0.004	<0.4**		57.4 ± 12.3	0.210**	0.76

[a] The fast local motions are ill resolved. The values of associated amplitudes are calculated assuming a limiting anisotropy value of (*) 0.225 and (**) 0.210, respectively.

now make up about 35% of the anisotropy decay. The N-terminal region becomes even more flexible in des-1,2-AMPA as the global protein motions make up only about half of the anisotropy decay. Furthermore, an intermediate correlation time of about 1.0–1.5 ns is also observed. The behavior of des-1,2-AMPA is in fact similar to the more flexible pro-PLA2 (Ludescher et al., 1988) and of Trp-31 in the mutant PLA2 (Kuipers et al., 1991). These results suggest that deletion of Ala-1 does not completely disrupt the organization of the N-terminal region, although deletion of Leu-2 does disrupt the conformational intengrity of the N-terminal region in the E form. A similar sequential increase in the conformational disorder in the N-terminal region due to these deletions has been observed by photo-CIDNP and immunological assays (Van Scharrenburg et al., 1982, 1984b).

Results from the anisotropy decay measurements of the E*I form on DTPM vesicles are also summarized in Table 7. The anisotropy decays of the bound PLA2, unlike in solution could be described by one correlation time of about 30 ns as the associated amplitude represents more than 95% of the limiting anisotropy value. As the recovered zero-time anisotropy value of 0.21 (at 295 nm) is similar to that of the frozen tryptophan residue (Valeur & Weber, 1977), there are no fast unresolved motions in this system. The correlation time of 30 ns is, however, significantly smaller than that expected for the global motions of a particle of the size of a small lipid vesicle. These parameters for the Trp-3 anisotropy decays in the case of the bound enzyme compare favorably with the values observed for extrinsic probes on fluid bilayers (Lakowicz et al., 1985; Maliwal et al., 1986), and they are consistent with the observation that in the presence of PLA2 the DTPM bilayer is in the fluid phase (Jain et al., 1986c).

The anisotropy decays of Trp-3 in the E*L (DTPM) form of des-1-AMPA were similar to those for PLA2 as the global motions still accounted for about 87% of the total anisotropy. Trp-3 of des-1,2-AMPA in the E*I form is somewhat more flexible as about 25% of the anisotropy decay was associated with the local motions. Overall, the anisotropy decay results suggest that the segmental motions of the N-terminal region are significantly dampened in the E*I form of PLA2 and its deletion mutants. Furthermore, rigidification of the N-terminal region of the enzyme at the interface in the presence of a high-affinity ligand does not depend on the presence of Ala-1.

DISCUSSION

The catalytic and interfacial recognition functions of PLA2 are independent. Since they are related by the sequential equilibria, quantitative dissection of the underlying processes has not been possible in most published studies. The protocols described here dissect the functional contribution of the three sequential equilibria: E to E*, E* + S to E*S, and E*S to E* + P. In conjunction with the knowledge of the primary rate and equilibrium parameters, such information can provide insights into the behavior of PLA2 under more complex situations where quantitative analysis is not possible yet due to an inadequate understanding of the underlying variable. Although the primary conclusions developed here are based on some of the studies at anionic interfaces, the conclusions are valid for the events at the zwitterionic as well as the anionic interface. This has been demonstrated under a variety of conditions (Berg et al., 1991; Jain et al., 1991a; Ghomashchi et al., 1991), and the reason for this is rather straightforward. On the basis of virtually all of the detailed kinetic studies carried out so far, it may be emphasized that the primary rate and equilibrium parameters for the interfacial catalytic cycle of PLA2 do not depend on the charge and organization ("quality") of the interface (Berg et al., 1991). On the other hand, the charge and organization of the interface have a significant effect on the E to E* equilibrium. Such effects of the quality of the interface are particularly accentuated under the conditions where the E to E* equilibrium is largely in the favor of the E form as is often the case at zwitterionic interfaces as discussed below.

Results with mutants summarized in Table 1 show that the various substitutions have little effect on the overall catalytic turnover on DMPM vesicles, and therefore it may be concluded that the effect on the underlying rate and equilibrium parameters is marginal, if any. On the other hand, mutants with deletions at the N-terminus, such as des-1-AMPA, exhibit a significant decrease in the affinity for the catalytic site directed ligands without any significant effect on the chemical step or on the affinity for the anionic interface. Additional implications of the analysis described in this paper are considered below.

(a) A key feature of interaction of PLA2 with interfaces is that the E to E* equilibrium is not favored at zwitterionic interfaces; the K_d values are about 1 mM. However, on an anionic interface the overall equilibrium is shifted in the favor of the bound enzyme (Jain et al., 1982; Ghomashchi et al., 1991) with K_d values of <10 μM. A significant part of the loss of activity of the modified PLA2 on zwitterionic interfaces (Slotboom & de Haas, 1975; Van Scharrenburg et al., 1984a,b) can be attributed to the inability of these enzymes to bind to zwitterionic interfaces. For example, the Ala-1 substitution mutants which showed little activity with zwitterionic substrates are fully catalytically active at anionic interfaces (Jain et al., 1986b, and results in Table 1) to which these enzymes can bind readily.

(b) The overall equilibrium would also shift toward the bound forms of the enzyme (E* and E*L) if an active site directed ligand is present at the interface. The difference

between the K_d and K_d^I values summarized in Table 3 are good examples (for additional considerations, see Jain et al., 1993). This aspect is further emphasized by the behavior of des-1-AMPA, which does not bind to hexadecylphosphocholine micelles (Van Scharrenburg et al., 1984b). Besides providing the interface for the binding of the enzyme, hexadecylphosphocholine also binds to the active site of PLA2 with a K_I^* = 0.65 mole fraction (Jain et al., 1991c). Thus the reported apparent K_d value of about 0.15 mM for hexadecylphosphocholine micelle also has contributions from the E*L form (60%) as indicated by the K_d value of about 0.6 mM for the His-48-modified PLA2 (Pieterson et al., 1974). Any increase in the K_I^* value would also lead to a significantly higher apparent K_d, as is probably the case with the deletion mutants.

(c) Since des-1-AMPA does not bind to deoxy-LPC micelles (up to 6 mM), it would suggest that the intrinsic interfacial binding affinity of PLA2 for zwitterionic interface is indeed affected by the deletion of Ala-1. Here the underlying assumption is that deoxy-LPC is a "perfect" neutral diluent without any affinity for the catalytic site of the bound enzyme. This may be justified because the K_d value for PLA2 is essentially identical to that of PLA2 methylated at His-48 (Jain et al., 1991a). Thus it may be argued that Ala-1 does play a role in the binding of the enzyme to zwitterionic interfaces.

(d) In case of the snake venom PLA2, modification of the amino group at the N-terminus to a keto group results in a 10-fold lower affinity for zwitterionic micelles (Verheij et al., 1981). Since the bound enzyme does not hydrolyze dioctanoylglycerophosphocholine micelles, it may be suggested that the N-terminal residue also plays a role in the E* to E*S step, i.e., K_S^* is altered.

Results reported in this paper also bear on the functional role of the N-terminal region of PLA2 and ultimately to the structural basis for interfacial activation. From the weight of the experimental evidence summarized in the introduction section and developed in this paper, it is now clear that the hydrogen-bond network associated with residues 52 and 72 as well as that involving the α-NH_3^+ of Ala-1 and Gln-4 is not essential for the chemical step. The functional role of the hydrogen-bond network is not clear yet; however, it is quite possible that the network is the result of the exposure of the hydrophobic surface of the protein to bulk water and that it is substituted by the groups from the interface in the E*L complex.

Unlike substitutions involving α-NH_3^+ of Ala-1, its deletion resulted in a 60% decrease in v_o, and the affinity for the active site directed anionic ligands decreases by 90%. This decrease in the affinity could result from one or more of the following factors: (i) We know that the N-terminal region is more disordered in the E form, which will effectively reduce the population of the conformers with a higher affinity for the ligand. (ii) In des-1-AMPA, Trp-3 is in a more polar environment, indicating an incomplete desolvation of the microinterface necessary for the formation of the E*I complex. (iii) Residues Leu-2 and Phe-5 are a part of the wall of the active-site cavity for the binding of the ligands (Scott et al., 1990; Thunnissen et al., 1990). The expected perturbation of the N-terminal segment in the deletion mutants will reduce the stability of the complex. (iv) Subtle differences between PLA2 and deletion mutants are consistent with the possibility that desolvation involves several steps. This interpretation is also consistent with other results. In case of pro-PLA2 the interfacial desolvation is either incomplete or does not occur at all (Jain & Vaz, 1987), and therefore, a similar shift in the E* to E*S equilibrium can be expected. Higher polarity of the substrate binding cavity has also been shown to lower the interfacial activity of Phe-5-Tyr (Van Scharrenburg et al., 1982) and Phe-106-Tyr (Dupureur et al., 1992b) mutants. Additional factors are also at work as implicated by the observation that K_S^* for the Tyr-52-Ala mutant is increased, predominantly by an increase in the dissociation of the E*S complex, i.e., the k_{-1} step (Dupureur et al., 1992).

In pro-PLA2 the N-terminal segment is disordered. In PLA2, formed by proteolytic cleavage of the heptapeptide from pro-PLA2, the hydrogen-bond network is formed and the N-terminal segment becomes rigid (Dijkstra et al., 1981, 1983). The N-terminal segment provides parts of the interfacial binding region (Trp-3, Arg-6) as well as some of the contacts of the substrate binding site (Leu-2, Phe-5, Ile-9). The motions of Trp-3 therefore reflect not only the motional freedom of the indole ring but also the rigidity of the N-terminal segment and the associated structures. Two trends are obvious from the anisotropy decays. The limited flexibility of the N-terminal region in the E form helps to maintain an appropriate interfacial binding region, and its disorder leads to a loss of affinity for zwitterionic interfaces. Furthermore, the fluorescence intensity decays suggested that the E* form with its dampened N-terminal segmental motions is most likely a narrower ensemble of conformers. It is possible that these E* conformers have a higher affinity for the substrate. What is surprising is that even in the case of des-1-AMPA, which has some conformational disorder in solution, binding of a high-affinity ligand at the interface is able to rigidify the N-terminal segment. A similar decrease in the conformational disorder induced by high-affinity ligands has been observed for zymogens of serine proteases (Vijayan & Salunke, 1984). It may be recalled that these proteases are also formed by proteolytic cleavage of a peptide from the N-terminus of zymogens.

Taken together, these observations reinforce the notion, based on the molecular dynamics calculations on the crystallographic results (Sessions et al., 1988; Gros et al., 1990) and the NMR studies (Dekker et al., 1991a), that the N-terminal region of PLA2 exists as an ensemble of isoenergetic conformations separated by low-energy barriers. The role of such closely related structures could be to facilitate suitable molecular contacts of the interfacial binding region on the enzyme with the substrate interface where it is in direct contact with as many as 40 phospholipid molecules (Volwerk & de Haas, 1982; Jain et al., 1982, 1986a–c). Since the precise organization of the interface differs from one substrate to another, it appears reasonable that a flexible arrangement of the amino acid residues in the interfacial binding region would promote the optimal arrangement of the interacting groups at the entrance to the catalytic site that is energetically and kinetically favorable for the transfer of the substrate to the active site. We further suggest that as the bound water molecules and the hydrogen-bond network represent multiple intramolecular contacts involving several types of low-energy interactions. These may be required to couple the removal of bound water molecules and the reorganization of the hydrogen bonds with the desolvation of the microinterface. The ΔG for the removal of a phospholipid monomer from a vesicle to the aqueous phase is >20 kcal/mol. Thus a change in the polarity of the microinterface due to desolvation would shift the E* to E*S equilibrium for the bound enzyme. The dehydration of the lipid–protein interface and the active site therefore not only makes an entropic contribution to the binding process (E to E*), but also facilitates the diffusion of

lipid monomers from the vesicles to the active site (E* to E*S).

To recapitulate, results reported in this paper essentially rule out an obligatory role of the H-bond network involving α-NH_3^+ of Ala-1 in the chemical step of the catalytic cycle. These results also call in question ideas about "interfacial activation" as invoked by the "conformational theory" (Volwerk & de Haas, 1982; Peters et al., 1992) which requires definite positioning of the α-NH_3^+ group of Ala-1 in the overall "active" conformation of PLA2. On the other hand, a role of the N-terminus in the substrate binding to the active site would be consistent with the K-type of interfacial activation of PLA2 (Jain et al., 1993), according to which the affinity of the E* form of PLA2 for the active site directed ligands is considerably higher than it is for the E form of the enzyme. The structural basis for the K-type of activation is indicated in the desolvation tendency of the microinterface rather than in a conformational change in the enzyme.

REFERENCES

Berg, O. G., Yu, B.-Z., Rogers, J., & Jain, M. K. (1991) *Biochemistry 30*, 7283–7297.

Dekker, N., Peters, A. R., Slotboom, A. J., Boelens, R., Kaptein, R., & de Haas, G. H. (1991a) *Biochemistry 30*, 3135–3147.

Dekker, N., Peters, A. R., Slotboom, A. J., Boelens, R., Kaptein, R., Dijkman, R., de Haas, G. H. (1991b) *Eur. J. Biochem. 199*, 601–607.

Dijkstra, B. W., Kalk, K. H., Hol, W. G. J., & Drenth, J. (1981) *J. Mol. Biol. 147*, 97–123.

Dijkstra, B. W., Renetseder, R., Kalk, K. H., Hol, W. G. J., & Drenth, J. (1983) *J. Mol. Biol. 168*, 163–179.

Donovan, J. W. (1969) in *Physical Principles and Techniques of Protein Chemistry* (Leach, S. J., Ed.) Part A, pp 101–170, Academic Press, New York.

Dupureur, C. M., Yu, B.-Z., Jain, M. K., Noel, J. P., Deng, T., Li, Y., Byeon, I. L., & Tsai, M. D. (1992a) *Biochemistry 31*, 6402–6413.

Dupureur, C. M., Yu, B.-Z., Mamone, J. A., Jain, M. K., & Tsai, M. D. (1992b) *Biochemistry 31*, 10576–10583.

Ghomashchi, F., Yu, B. Z., Berg, O. G., Jain, M. K., & Gelb, M. H. (1991) *Biochemistry 30*, 7318–7329.

Gros, P., van Gunstern, W. F., & Hol, W. G. J. (1990) *Science 249*, 1149–1152.

Jain, M. K., & Maliwal, B. P. (1985) *Biochim. Biophys. Acta 814*, 134–140.

Jain, M. K., & Vaz, W. L. C. (1987) *Biochim. Biophys. Acta 905*, 1–8.

Jain, M. K., & Maliwal, B. P. (1993) *Biochemistry 32*, 11838–11846.

Jain, M. K., Egmond, M. R., Verheij, H. M., Apitz-Castro, R. J., Dijkman, R., & de Haas, G. H. (1982) *Biochim. Biophys. Acta 688*, 341–348.

Jain, M. K., Rogers, J., Jahagirdar, D. V., Marecek, J. F., & Ramirez, F. (1986a) *Biochim. Biophys. Acta 860*, 435–447.

Jain, M. K., Maliwal, B. P., de Haas, G. H., & Slotboom, A. J. (1986b) *Biochim. Biophys. Acta 860*, 448–461.

Jain, M. K., Rogers, J., Marecek, J. F., Ramirez, F., & Eibl, H. (1986c) *Biochim. Biophys. Acta 860*, 462–474.

Jain, M. K., Rogers, J., & de Haas, G. H. (1988) *Biochim. Biophys. Acta 940*, 51–62.

Jain, M. K., Yu, B.-Z., Rogers, J., Ranadive, G. N., & Berg, O. G. (1991a) *Biochemistry 30*, 7306–7317.

Jain, M. K., Rogers, J., Berg, O., & Gelb, M. H. (1991b) *Biochemistry 30*, 7340–7348.

Jain, M. K., Tao, W., Rogers, J., Arenson, C., Eibl, H., & Yu, B.-Z. (1991c) *Biochemistry 30*, 10256–10268.

Jain, M. K., Yu, B.-Z., & Berg, O. G. (1993) *Biochemistry, 32*, 11319–11329.

Johnson, M. L. (1983) *Biophys. J. 44*, 101–106.

Kuipers, O. P., Dekker, N., Verheij, H. M., & de Haas, G. H. (1990) *Biochemistry, 29*, 6094–6102.

Kuipers, O. P., Vincent, M., Brochon, J., Verheij, H. M., de Haas, G. H., & Gallay, J. (1991) *Biochemistry 30*, 8771–8785.

Laczko, G., Gryczynski, I., Gryczynski, Z., Wiczk, W., Malak, H., & Lakowicz, J. R. (1990) *Rev. Sci. Instrum. 61*, 2331–2337.

Lakowicz, J. R., Laczko, G., Cherek, H., Gratton, E., & Limkeman, M. (1984) *Biophys. J. 46*, 463–477.

Lakowicz, J. R., Cherek, H., Maliwal, B. P., & Gratton, E. (1985) *Biochemistry 24*, 376–383.

Ludescher, R. D., Volwerk, J. J., de Haas, G. H., & Hudson, B. S. (1985) *Biochemistry 24*, 7240–7249.

Ludescher, R. D., Johnson, I. D., Volwerk, J. J., de Haas, G. H., Jost, P. C., & Hudson, B. S. (1988) *Biochemistry 27*, 6618–6628.

Lumry, R., & Hershberger, M. (1978) *Photochem. Photobiol. 27*, 819–840.

Maliwal, B. P., & Lakowicz, J. R. (1986) *Biochim. Biophys. Acta 873*, 161–172.

Maliwal, B. P., Hermetter, A., & Lakowicz, J. R. (1986) *Biochim. Biophys. Acta 873*, 173–181.

Peters, A. R., Dekker, N., van den Berg, L., Boelens, R., Kaptein, R., Slotboom, A. J., & de Haas, G. H. (1992) *Biochemistry 31*, 10024–10030.

Pieterson, W. A., Vidal, J. C., Volwerk, J. J., & de Haas, G. H. (1974) *Biochemistry, 13*, 1455–1460.

Ramirez, F., & Jain, M. K. (1991) *Proteins 9*, 229–239.

Scott, D. L., White, S. P., Otwinowski, Z., Yuan, W., Gelb, M. H., & Sigler, P. B. (1990) *Science 250*, 1541–1546.

Sessions, R. B., Dauber-Osgnthorpe, P., & Osgnthorpe, D. J. (1988) *J. Mol. Biol. 209*, 617–633.

Slotboom, A. J., & de Haas, G. H. (1975) *Biochemistry 14*, 5394–5399.

Steiner, R. F., & Kirby, E. P. (1969) *J. Phys. Chem. 73*, 4130–4135.

Thunnissen, M. M. G. M., Ab, E., Kalk, K. H., Drenth, J., Dijkstra, B. W., Kuipers, O. P., Dijkman, R., de Haas, G. H., & Verheij, H. M. (1990) *Nature 347*, 689–691.

Valeur, B., & Weber, G. (1977) *Photochem. Photobiol. 25*, 441–444.

Van Dam-Mieras, M. C. E., Slotboom, A. J., Pieterson, W. A., & de Haas, G. H. (1975) *Biochemistry 14*, 5387–5394.

Van Scharrenburg, G. J. M., Pujik, W. C., Egmond, M. R., Van der Schaft, P. H., de Haas, G. H., & Slotboom, A. J. (1982) *Biochemistry 21*, 1345–1352.

Van Scharrenburg, G. J. M., Pujik, W. C., Seeger, P. R., de Haas, G. H., & Slotboom, A. J. (1984a) *Biochemistry 23*, 1256–1263.

Van Scharrenburg, G. J. M., Jansen, E. H. J. M., Egmond, M. R., de Haas, G. H., & Slotboom, A. J. (1984b) *Biochemistry 23*, 6285–6294.

Van Scharrenburg, G. J. M., Slotboom, A. J., de Haas, G. H., Mulqueen, P., Breen, P. J., & Horrocks, W. W. (1985) *Biochemistry 24*, 334–339.

Verheij, H. M., Slotboom, A. J., & de Haas, G. H. (1981) *Rev. Physiol. Biochem. Pharmacol. 91*, 91–203.

Vijayan, M., & Salunke, D. M. (1984) *J. Biosci. 6*, 357–377.

Volwerk, J. J., & de Haas, G. H. (1982) in *Lipid Protein Interactions* (Jost, P. C., & Griffith, O. H., Eds.) Vol. 1, pp 69–149, John Wiley & Sons, New York.

Weber, G. (1977) *J. Chem. Phys. 66*, 4081–4091.

Yu, B.-Z., Berg, O. G., & Jain, M. K. (1993) *Biochemistry 32*, 6485–6492.